Journal of Hazardous Materials 361 (2019) 348–356

Contents lists available at ScienceDirect

Journal of Hazardous Materials

journal homepage: www.elsevier.com/locate/jhazmat

Development and characterization of yttrium-ferric binary composite for treatment of highly concentrated arsenate wastewater

Ling Yu[a,b,1], Yang Yu[a,c,1], Jingyi Li[a], J. Paul Chen[a,*]

[a] Department of Civil and Environmental Engineering, National University of Singapore, 10 Kent Ridge Crescent, 119260, Singapore
[b] School of Environmental Science and Engineering, Sun Yat-Sen University, Guangzhou, 510006, China
[c] Guangdong Key Laboratory of Environmental Pollution and Health, and School of Environment, Jinan University, Guangzhou, 510632, China

GRAPHICAL ABSTRACT

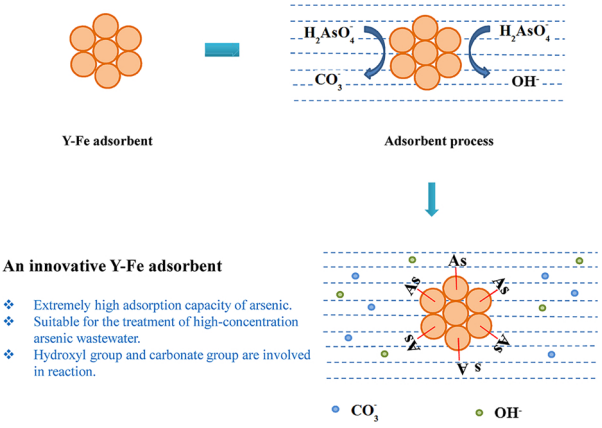

ARTICLE INFO

Keywords:
Arsenate
Yttrium-ferric composite
Adsorption
Hydroxyl group
Carbonate group

ABSTRACT

Highly concentrated arsenic generated from industrial operation processes has posted a great thrust to humans. In this study, yttrium-ferric binary composite prepared through a simple co-precipitation method and applied for removing highly concentrated arsenic from the simulated arsenic-containing water. An optimal molar ratio of Y/Fe was determined as 8:1, which had a point of zero charge of around 7.0. The yttrium-ferric binary composite was aggregated by the nano-sized particles. The chemical state of yttrium and iron in the adsorbent was + III. The maximum adsorption capacities of the adsorbent towards arsenate (As(V)) were 401.8 mg-As/g at pH 4 and 288.7 mg-As/g at pH 7, respectively. A contact time of 8 h was sufficient to achieve 80% of the ultimate removal, faster than many reported/commercial water treatment materials. The existence of fluoride and phosphate ions significantly retarded the uptake of arsenic, indicating that likely the adsorbent was capable of adsorbing both contaminants. The mechanism study with several tools such as X-ray photoelectron spectroscopy (XPS) indicated that such functional groups as hydroxyl and carbonate groups participated in the As(V) adsorption process via ligand exchange followed by the inner-sphere complexation.

* Corresponding author.
E-mail address: jpaulchen@icloud.com (J.P. Chen).
[1] Co-first authorship.

https://doi.org/10.1016/j.jhazmat.2018.07.068
Received 3 April 2018; Received in revised form 4 July 2018; Accepted 17 July 2018
Available online 23 July 2018

1. Introduction

Arsenic is a naturally occurring element and has been regarded as one of first priority contaminants in drinking water because of its carcinogenicity, high toxicity and great bioaccumulation. The maximum contaminant level (MCL) of arsenic in drinking water was set at 10 μg/L by the United States Environmental Protection Agency (USEPA) in 2006.

Especially in recent decades, human activities such as liquid-crystal display (LCD) production, mining, and agricultural work and have caused arsenic contamination to become a severe environmental problem. The wastewater from some operational units in above industries contains extremely high concentrations of arsenic ranging from a few mg/L to several thousands of mg/L, which is fatal to humans. Arsenic from such wastewater can enter our water environment if it is not appropriately managed. For example, a location at the Yangzonghai Lake in China had the arsenic concentration of 23.92 mg/L, which is more than 23 thousand times higher than the MCL (USEPA) [1]. In addition, the naturally occurring arsenic in the groundwater in some areas has posted a notable risk to humans in both developing countries including Bangladesh, China, India and Vietnam and developed countries such as Canada and United States.

Adsorption is recognized as the most promising technology among handful available technologies due to its operation simplicity, great flexibility, and cost-effectiveness. Therefore, various adsorbents have been fabricated for removing arsenic from water. However, the technology in general has several drawbacks including low removal efficiency of available adsorbents and severe interference by complex solution properties (e.g., solution pH and the existence of competitive anions), which limit its applications in the treatment, in particular for arsenic-rich wastewater treatment. Thus, more efforts need to be devoted to developing more effective and economical adsorbents for arsenic removal.

Recently, several adsorbents synthesized from rare-earth metals have attracted wide attentions because of their excellent performance on the removal of anionic contaminants [2–4]. Such trivalent rare-earth elements as zirconium, lanthanum and cerium have been utilized in the fabrication of adsorbents that are successful in removal of arsenic [5].

Yttrium, an element with the chemistry similar to the aforementioned, has shown its great application potential on the effective adsorption of arsenic. A basic yttrium carbonate was used for arsenic removal from aqueous solution [6]. Lack of stability at lower pH hindered its industrial applications, although it worked well in the removal of both arsenate and arsenite. Developing the yttrium-based adsorbent in the form of hydroxide would be a better solution for improving its stability in acidic conditions. The materials synthesized through combining rare-earth metal(s) with relatively abundant and low-cost heavy metal salts (e.g. iron) can enhance the adsorption performance [4,7]. Meanwhile, the cost of prepared adsorbents can greatly be reduced. A recently reported magnetic ferrum-yttrium binary oxide can maximally remove 200 mg of arsenic per gram of adsorbent from water at pH 5 [8].

To promote yttrium-based adsorbents for industrial-scale operations in treatment of highly As(V)-contaminated water, more R&D work is of great importance, especially on better adsorption performance at both acidic and neutral conditions, which is the bottleneck for the efficient removal of anionic contaminants.

In this study, an optimized yttrium-ferric adsorbent was synthesized through a facile co-precipitation approach. The field emission scanning electron microscopy (FESEM) analysis was conducted to observe the surface morphology of the virgin adsorbent. Several batch adsorption experiments were carried out to investigate the adsorption kinetics and isotherm, and the influences of solution pH, ion strength and competitive substances on the uptake. A XPS study on the adsorbent was conducted so as to reveal the possible adsorption mechanisms.

2. Materials and methods

2.1. Materials

The chemicals used in the fabrication of adsorbent and the adsorption studies were $Y(NO_3)_3{\cdot}6H_2O$, $Fe(NO_3)_3{\cdot}9H_2O$ and $Na_2HAsO_4{\cdot}7H_2O$, which were of reagent grade. These chemicals, the humic acid sodium salt (HA), the competitive substances, and the common acid/base used for pH adjustment were all purchased from Sigma-Aldrich.

The As(V) stock solution of 1000 mg/L was first prepared by dissolving $Na_2HAsO_4{\cdot}7H_2O$ in the DI water. Each working solution was freshly prepared by diluting the 1000-mg/L As(V) stock solution with the DI water.

2.2. Adsorbent preparation

The Y-Fe binary oxide adsorbents with different molar ratios of Y^{III} and Fe^{III} were synthesized. First, $Y(NO_3)_3{\cdot}6H_2O$ and $Fe(NO_3)_3{\cdot}9H_2O$ were dissolved in the DI water under being stirred for 2 h. Afterward, 1-M NaOH was added dropwise to the mixture until the pH reached 8, at which the precipitate was formed. The suspension was then sonicated for 40–60 min and continued to be stirred for another 2 h.

The obtained precipitate was separated by a centrifuge. The particles (precipitate) were rinsed for 5 times by the DI water, which were then dried in an oven at 80–90 ℃ overnight. Finally, fine particles (< 100 μm) after grinding and sieving were used for the adsorption studies.

The adsorption performances of adsorbents with different Y/Fe molar ratios were tested first with the result given in Fig. 1. The adsorbent with the Y/Fe molar ratio at 8:1 was finally chosen in subsequent experiments to investigate the adsorption behavior and the mechanism.

2.3. Characterization of adsorbent

The FESEM (JSM6700 F, JEQ, Japan) was applied to study the surface morphology of the adsorbent (the sample was coated with a thin platinum film). The point of zero charge (pH_{PZC}) was measured according to the literature summarized as follows [9,10]. The particle was first added in 0.01-M $NaNO_3$ for 24 h so that the pH became constant. The NaOH or HNO_3 solution was used to adjust the pH of the mixture to certain values in different containers. After be stirred for 1 h, the initial pH was measured by a pH meter (Orion Star A211). 1.5-g $NaNO_3$ was then added to each container to keep the final electrolyte concentration

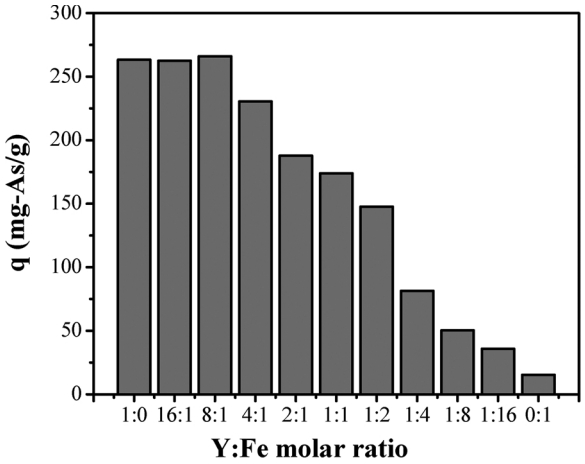

Fig. 1. Adsorption capacities of Y-Fe binary oxide composites with different molar ratios of Y/Fe. (m = 0.1 g/L; $[As]_0$ = 50 mg/L; pH = 7.0; contact time = 48 h).

at about 0.45 M. The suspension was agitated for another 3 h and the final pH was measured. The results were processed by plotting ΔpH (final pH - initial pH) versus final pH. The pH_{PZC} of the adsorbent was the pH value, where ΔpH equals to 0.

2.4. Adsorption experiments

The arsenic containing water with a concentration as high as 100 mg/L was used to simulate that in such industrial operations as the LCD production. A study on the adsorption kinetics was conducted in order to find out the reaction rate and equilibrium time of the adsorption process. The effects of such important chemical parameters of pH, initial arsenic concentration, existence of competitive substances and adsorbent dosage on the removal were studied. The experiments were all conducted on a shaker at 200 rpm at the room temperature. The concentration of As(V) was measured by an inductively coupled plasma optical emission spectrometer (ICP-OES, Thermo iCAP 6000). All the experiments were conducted at least three times and the averaged results are provided in this paper.

The experiment on the adsorption kinetics was carried out with an initial As(V) concentration ($[As]_0$) of 30 mg/L and the adsorbent dosage (m) of 0.1 g/L. The solution pH was controlled constantly at 7.0 throughout the course of experiment by adding NaOH or HNO_3. The water samples were collected after being filtered by 0.45 μm Nylon syringe filters and the concentrations were determined by the ICP-OES.

Two sets of experiments for the pH-effect study were conducted; the initial As(V) concentration was 50 mg/L and the adsorbent dosage was 0.1 g/L for both sets. In the first set, solution pH values were maintained from 2 to 11 respectively throughout the experiment. In the second set, pH was just initially adjusted at 2 to 11 without further control during the adsorption process. The solutions of both studies were stirred for 24 h. The water samples were collected for the ICP-OES analysis.

An adsorption isotherm experiment was conducted with the initial As(V) concentration ranging from 1 to 100 mg/L. 0.1-g/L adsorbent was added to each arsenic solution. The pH was maintained at 7.0 throughout the course of study. Other experimental operation steps were the same as those of the pH effect experiment.

The natural organic matters, fluoride, sulfate, carbonate and phosphate well exist in different types of waters. As such, above substances were chosen to examine their influences on the As(V) uptake. The solutions were prepared respectively by adding each competitive substance into As(V) solution. The initial As(V) concentration was 30-mg/L; the concentrations of other substances were of three levels: 0.1, 1 and 10-mM for fluoride, carbonate, sulfate and phosphate and 1, 5 and 10-mg/L for HA. Afterward, the 0.1-g/L adsorbent was added into each solution; the solution pH was maintained at 7.0 during reaction period of 24 h. Other experimental steps were the same as those of the pH effect experiment.

Ionic strength may affect adsorption through a few mechanisms. In the ionic strength effect experiments, different amounts of sodium nitrate (as a representation of ionic strength) were added into 30-mg/L As (V) solutions which has pH adjusted at 7.0 and maintained throughout this experiment. The adsorbent dosage was 0.1 g/L. The subsequent steps were the same as the aforementioned.

To better understand the mechanism, an additional adsorption study was conducted with different dosages of the adsorbent at the initial As(V) concentration of 100 mg/L. The solution pH was initially adjusted at 8.0 and not controlled during the experiment. After the adsorption, the final pH and the concentration of carbonate in solution were measured by using the pH meter (Mettler Toledo, USA) and the total organic carbon analyser (Shimadzu TOC-5000, Japan), respectively. The values of inorganic carbon (IC) from the TOC analysis was used as the concentrations of carbonate. The arsenic concentrations were measured by the ICP-OES. The relationships between the contents of hydroxide/carbonate ions released from the adsorbent and those of As(V) adsorbed were established so as to find the roles of both hydroxide and carbonate on the arsenic uptake.

2.5. Spectroscopic analysis

The surface elemental composition of adsorbents was characterized by XPS (Kratos XPS system-Axis His-165 Ultra, Shimadzu, Japan). The detection limits were in the range of parts per thousand ranges [11]. The XPS machine is equipped with monochromatized AlKα X-ray source (1486.71 eV) and works at 150 W, 15 kV, 10 mA and analytical chamber base pressure of 3×10^{-8} Torr.

The calibration by the reference graphitic carbon at a binding energy of 284.8 eV was performed for all spectra to compensate for the charging effect during the analysis. The spectra of yttrium, iron, arsenic, carbon and oxygen were further processed by deconvolving with the subtraction of a linear background and a Gaussian (20%)-Lorentzian (80%) mixed function.

The high-resolution XPS spectra were processed by the XPSPEAK41 Software, a non-linear least-squares curve fitting program. The data obtained were used in the illustration of mechanisms for the arsenic binding onto the adsorbent.

3. Results and discussion

3.1. Selection of Y/Fe molar ratio

Different molar ratios of Y/Fe were used to prepare the composite adsorbents and the adsorption capacities of individual composites towards As(V) are shown in Fig. 1. It can be observed that the adsorption capacity of the adsorbent is significantly enhanced with increasing the molar ratio of yttrium and reaches a plateau afterwards. The optimal molar ratio is found as 8:1; the adsorbent has the best adsorption performance of 266.15 mg-As/g at pH 7.0 when it was prepared at this ratio. With a further increase in the molar ratio of yttrium, there is no obvious change of the adsorption capacity. Thus, the yttrium-ferric adsorbent with Y/Fe molar ratio of 8:1 was chosen to test the adsorption performance and study the mechanism in the subsequent experiments.

3.2. Adsorbent characterization

From the FESEM image as shown in Fig. 2a, we can see that the Y-Fe adsorbent is aggregated with numerous smaller particles in the size of several nanometers. The aggregation results in a porous structure of the adsorbent, which may facilitate the diffusion and adsorption of As(V).

The pH_{PZC} of the Y-Fe adsorbent is estimated as 7.0 according to Fig. 2b. The surface charge of the adsorbent is mainly dependent on solution pH. When pH is below its $pH_{PZC,}$ the adsorbent becomes positively charged, which is helpful in the uptake of As(V) anion due to favorable adsorption reactors and strong electrostatic attraction between the active sites and the anionic arsenic. However, the functional groups on the adsorbent for the uptake become less at $pH < pH_{PZC}$. In addition, repulsion force at such a pH can cause a negative effect on the removal. Therefore, it can be concluded that this adsorbent can better remove As(V) at pH lower than 7 (more discussion to be given in Section 3.4.1).

As shown in Fig. 3, the high-resolution XPS spectra of Y and Fe elements were decomposed to determine the valence states of the elements used in the adsorbent. According to positions of component peaks of Y 3d and Fe 2p spectra, the oxidation states of Y and Fe are + III.

3.3. Adsorption kinetics study

Fig. 4 shows that complete removal of As(V) can be achieved within 24 h and equilibrium adsorption capacity is 240 mg-As/g at pH 7.0. The

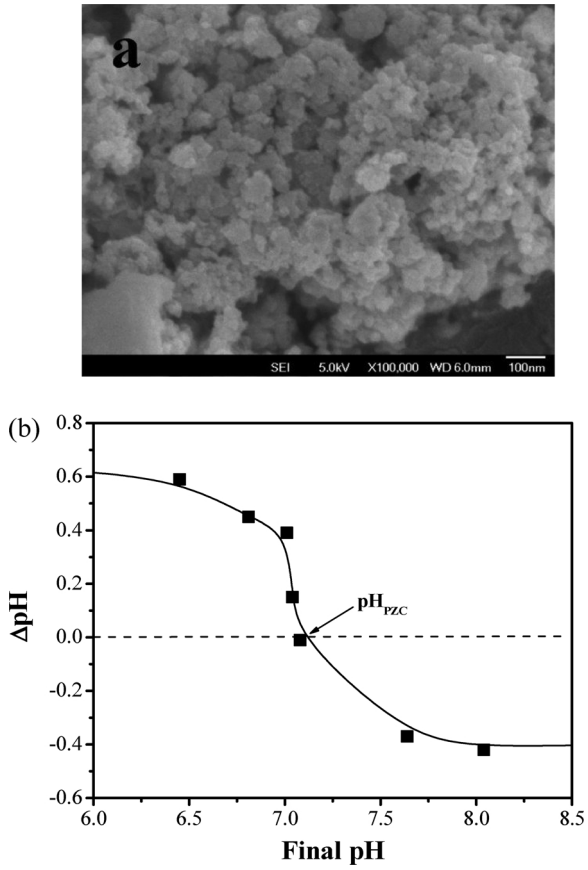

Fig. 2. Characterization of Y-Fe adsorbent: (a) FESEM image, and (b) point of zero charge.

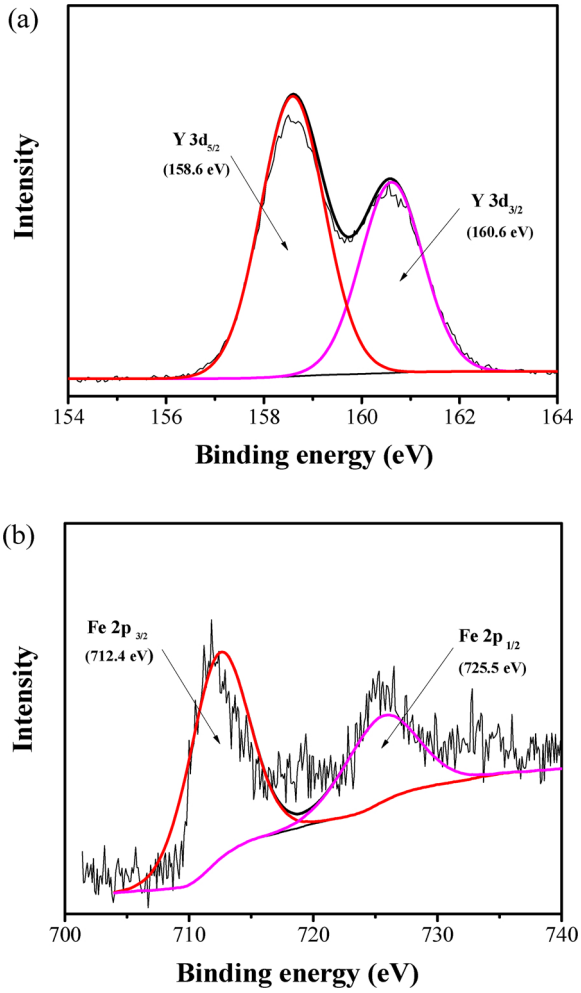

Fig. 3. XPS spectra of the Y-Fe adsorbent: (a) Y 3d, and (b) Fe 2p.

adsorption rate of As(V) is relatively rapid within the initial 4 h. It takes 8 h to achieve approximately 80% of the ultimate removal (200 mg-As/g at t = 8 h vs 240 mg-As/g at t = 24–28 h). Typically, the adsorption equilibrium of anionic contaminants such as fluoride and arsenic can be reached after a few days, for most of reported/commercial water treatment materials. As such, our adsorbent shows its advantage of relatively faster removal of anionic contaminants together with excellent adsorption capacity over many other adsorbents.

The experimental data were further fitted by the pseudo-first order, pseudo-second order and intraparticle diffusion models. As listed in Table 1, the pseudo-second order model fits the data better than the pseudo-first order model based on the correlation coefficient (r^2). This indicates that the uptake of As(V) is driven by chemisorption process.

Several previous studies demonstrated [12–14]: 1) if the plot of q_t against $t^{1/2}$ gives a straight line, intraparticle diffusion dominates the adsorption ; and 2) if the plot shows multi-linearity, two or more steps are involved in the adsorption kinetics. A larger value of α means a greater role of the surface adsorption in the rate-controlling step. If α equals to 0, the adsorption rate is limited by the intraparticle diffusion process [15]. According to values of k_{id} and α shown in Table 1, the adsorption process tends to be first governed by the intraparticle diffusion based on the linear portion. In the later adsorption stage, namely after 9 h, the adsorption rate slows down which may be due to the low As(V) concentration in aqueous phase [16].

3.4. Adsorption equilibrium study

3.4.1. pH effect

The higher uptake of As(V) occurs in pH 3 to 8 as shown in Fig. 5a. The maximum adsorption capacity of 316.35 mg-As/g is achieved at pH 4.0. A further increase in pH retards the adsorption. The adsorption of 277.58 mg-As/g can still be achieved at pH 7.0, far above most reported adsorbents listed in Table 3. The relatively low adsorption capacity at pH 2.0 and 3.0 is mainly due to the fact that the adsorbent becomes less stable under an acidic condition. At the pH range in this study, the major species of As(V) in solution are $H_2AsO_4^-$ and $HAsO_4^{2-}$ [17]. The functional groups on the adsorbent surface are strongly protonated and positively charged at pH < 7, which is beneficial in the adsorption reactions (e.g., interactions of hydroxide/carbonate with arsenic) and causes enhancement in electrostatic attraction between the adsorbent and arsenic species. Once the adsorbent surface becomes negatively changed at pH > 7, stronger electrostatic repulsion would occur and lead to the reduction in adsorption of As(V) [18]. Meanwhile, the competition between hydroxide and As(V) anions can be another reason to cause the remarkable reduction of As(V) uptake at basic condition.

Another pH-effect experiment was carried out, when the pH in the solution was not controlled throughout the adsorption process. The initial pH versus the final (equilibrium) pH is shown in Fig. 5b. After the adsorption, the equilibrium pH is found to be elevated, which is due to the release of hydroxide ions into the solution during the reaction. The increasing concentration of hydroxide ions in the solution would inhibit the further release of hydroxide from the adsorbent, leading to the decrease in adsorption at basic conditions.

The adsorption versus the initial pH is also illustrated in Fig. 5b. As the initial pH becomes increased, one can see that more adsorption occurs. When the initial pH ranges from 4 to 8 that is typical in water and wastewater, the arsenic uptake above 150 mg-As/g can be

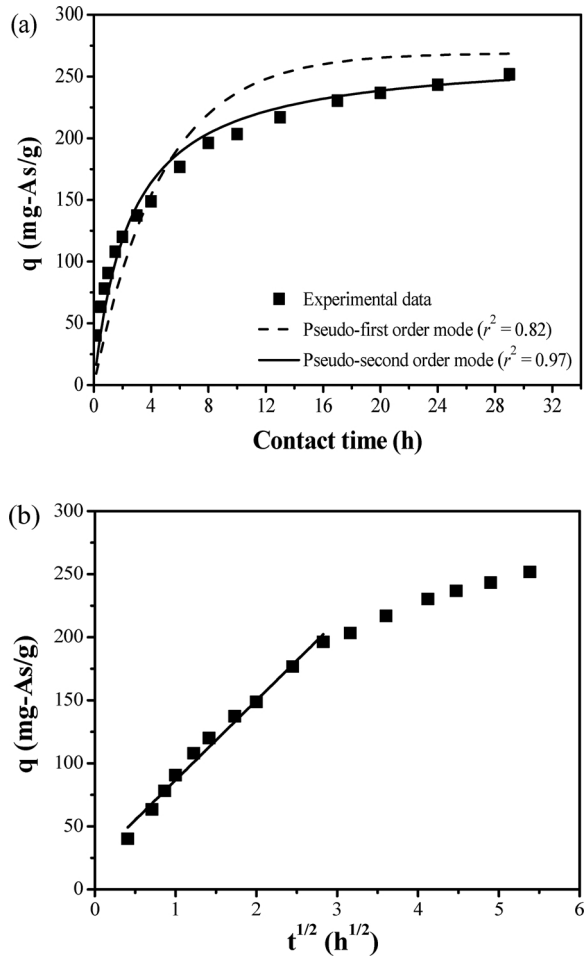

Fig. 4. Adsorption kinetics study of As(V): (a) experimental data and modeling results by the pseudo-first order and pseudo-second order models, and (b) the intraparticle diffusion model. (m = 0.1 g/L; $[As]_0$ = 30 mg/L; pH = 7.0).

obtained. This indicates potentially wider industrial applications for our material.

Although very low uptake of arsenic occurs at pH 11, we can take an advantage of that for the regeneration of spent adsorbent. One can use 0.1-M NaOH solution to regenerate the adsorbent for its recycle and reuse.

3.4.2. *Ionic strength effect*

The surface properties of the adsorbent may be affected by the ionic strength in water. The study of ionic strength effect can be used for identifying the type of surface complexes (e.g., the inner- and outer-sphere) formed between arsenic and the adsorbent [19]. If arsenic and active adsorption sites are weakly bonded, the adsorption is considered as outer-sphere ion-pair complexes. In contrast, the strong bonding often results in inner-sphere surface coordination complexes in which the uptake of As(V) is relatively insensitive to ionic strength [19,20]. As shown in Fig. 6, no obvious change of the adsorption capacity is observed with increasing ionic strength from 0 to 0.1 M. Therefore, the inner-sphere complexes should be formed during the adsorption

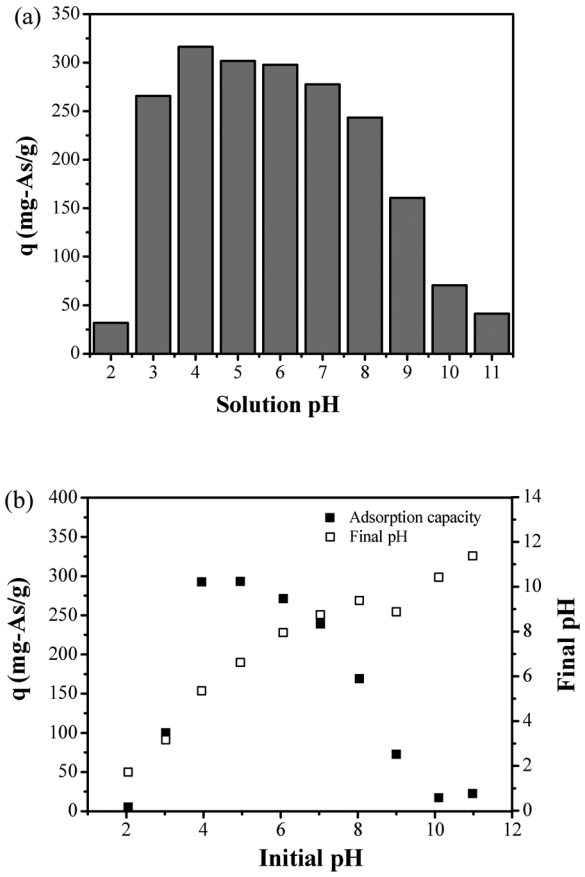

Fig. 5. pH effects on As(V) adsorption. (a) As(V) uptake with different pH, and (b) the initial pH versus equilibrium pH. (m = 0.1 g/L; $[As]_0$ = 50 mg/L; contact time = 24 h).

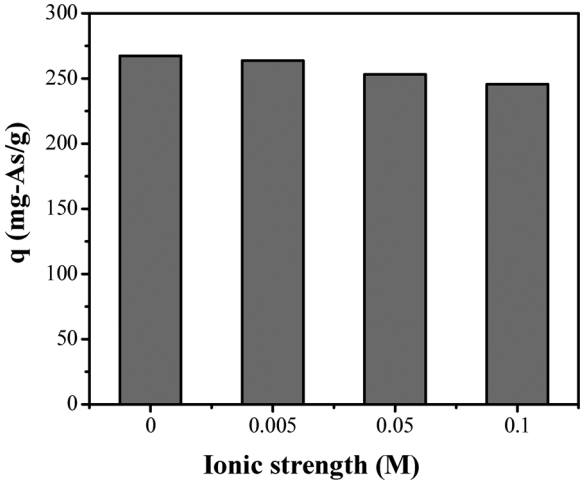

Fig. 6. Ionic strength effect on As(V) adsorption. (m = 0.1 g/L; $[As]_0$ = 30 mg/L; pH = 7.0; contact time = 24 h).

Table 1
Constants of adsorption kinetics models.

Pseudo-first order model			Pseudo-second order model			Intraparticle diffusion model		
K_1 (1/h)	q_e (mg/g)	r^2	K_2 ((g/mg)/h)	q_e (mg/g)	r^2	k_{id} ((mg/g)/$h^{1/2}$)	α (mg/g)	r^2
0.212	269.1	0.82	0.001	269.1	0.97	63.24	23.41	0.986

Table 2
List of parameters of Langmuir and Freundlich isotherms.

Solution pH	Langmuir isotherm			Freundlich isotherm		
	q_{max} (mg/g)	b (L/mg)	r^2	K ($mg^{(1-1/n)}L^{1/n}/g$)	$1/n$	r^2
pH 4	401.8	1.498	0.974	203.5	0.190	0.901
pH 7	288.7	0.810	0.937	151.3	0.016	0.860

process.

The finding is indeed important in the industrial applications. As industrial wastewater contains various inert ionic substances (represented as ionic strength), some commercial adsorbents and ion exchange resins do not perform well at different levels of ion strength. Our material performs well regardless of ionic strength level. This indicates that it will work well in treatment of industrial wastewater.

3.4.3. Adsorption isotherm study

The adsorption isotherm can provide fundamental physico-chemical information for deeply understanding the adsorption process. The adsorption isotherms of As(V) by the adsorbent were studied at optimum pH 4.0 and neutral pH 7.0. The Langmuir and Freundlich adsorption isotherms were both used to simulate the uptake process with the constants summarized in Table 2.

The maximum adsorption capacity of the adsorbent at pH 4.0 and 7.0 is 401.8 and 288.7 mg-As/g respectively as shown in Fig. 7, much higher than many other mixed metal adsorbents previously reported as illustrated in Table 3. The excellent performance of the adsorbent indicates its potential on the treatment of arsenic-rich industrial wastewater. Better adsorption performance at both acidic and neutral conditions and less requirement in dosage of adsorbent are of great importance in industrial wastewater treatment. The adsorbent after use can be removed by coagulation/sedimentation and filtration. Alternatively, it can be doped on supporting materials such as activated carbon for its applications.

As one can see from the correlation coefficients (r^2) from both models, the adsorption behavior can be better fitted by the Langmuir isotherm than the Freundlich isotherm under both pH conditions. The Langmuir isotherm is essentially for homogeneous/monolayer adsorption. The higher regression factor indicates that a homogeneous/monolayer adsorption of As(V) occurs.

3.4.4. Effect of competitive substances

As shown in Fig. 8, the influences of NOM and several key anions on the arsenic removal was studied. Only a slight decrease in the As(V) uptake occurs in the presence of sulfate, bicarbonate and HA. The uptake is significantly retarded by the existence of phosphate in solution due to the chemical similarity between arsenic and phosphate. As the concentration of phosphate in the solution is twice higher than arsenate concentration (0.4 mM), the adsorption of As(V) drops down by ~50%. The uptake of As(V) is also obviously hindered by the presence of fluoride (conc. of fluoride > 1 mM) owing to the intense competition of fluoride with As(V).

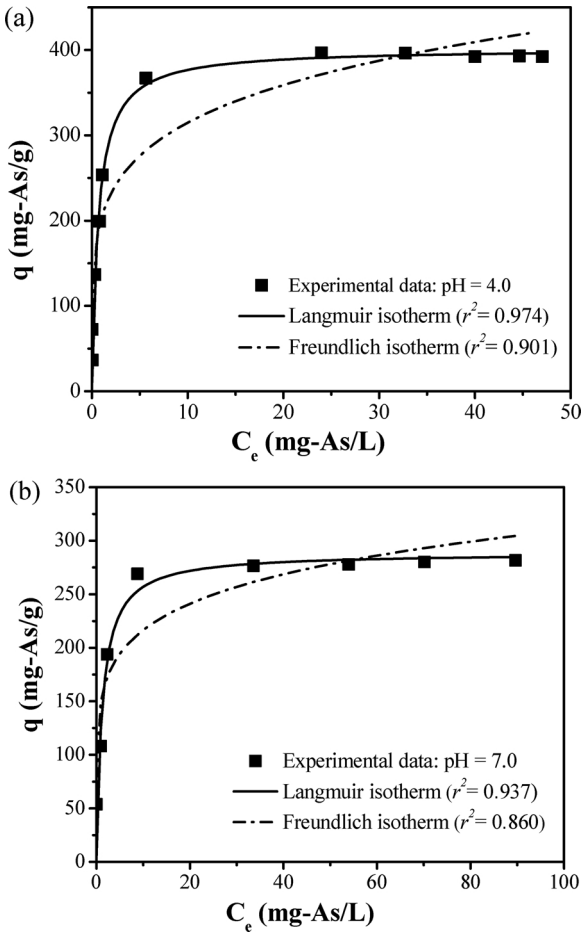

Fig. 7. Adsorption isotherms for As(V) removal at pH 4.0 and 7.0. (m = 0.1 g/L; contact time = 24 h).

To further study the intense competition of phosphate or fluoride with the arsenate anions, the related adsorption capacities of the adsorbent towards phosphate and fluoride were also measured. As listed in Table 4, the adsorbent exhibits a high adsorption affinity towards both phosphate and fluoride. The adsorption of phosphate and fluoride is respectively enhanced with increasing their concentrations, simultaneously leading to a severe reduction of As(V) uptake. This result confirms the intense competition between the arsenic and phosphate or fluoride. The adsorption capacity of the adsorbent towards phosphate and fluoride can respectively reach as high as 167.60 mg-P/g and 84.97 mg-F/g, suggesting that the adsorbent can be used for simultaneously removing As(V), phosphate and fluoride.

Table 3
Comparison of maximum As(V) adsorption capacities of different adsorbents.

Adsorbent	As(V) conc. (mg-As/L)	Max. As adsorption capacity (mg-As/g)	Experiment pH	Ref.
Fe-Cu binary oxide	0–60	82.7	7.0	[9]
Fe-Mn binary oxide	0–50	53.9	6.9	[21]
Fe-Zr binary oxide	5–40	26.6	7.0	[7]
Zr based nanoparticle	0–80	256.4	3.2	[22]
Mg-Al layered double hydroxide/GO composite	0–150	183.11	5.0	[23]
hydrous iron(III)-titanium(IV) bimetal mixed oxide	5–250	14.3	7.0	[24]
Fe_3O_4 coated boron nitrite nanotube	1–40	32.2	6.9	[25]
Y-Fe binary composite	0–100	288.7	7.0	Present study
		401.8	4.0	

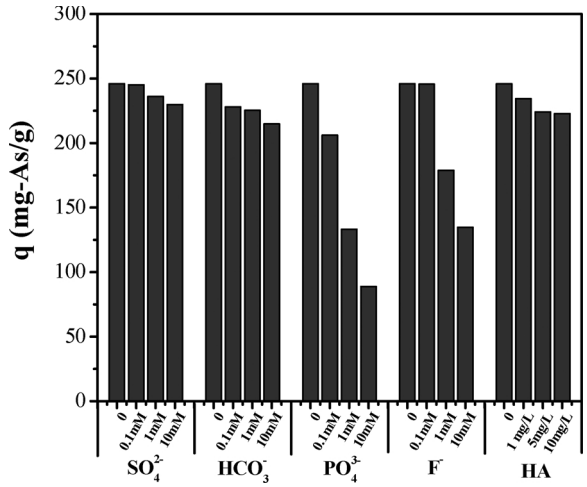

Fig. 8. Effects of HA and competitive anions on As(V) adsorption. (m = 0.1 g/L; $[As]_0$ = 30 mg/L (0.4 mM); solution pH = 7.0; contact time = 24 h).

3.5. Spectroscopic analysis

The interactions between the adsorbent and As(V) can be observed from the XPS wide scan spectra of the material before and after the uptake of arsenic. As shown in Fig. 9, the characteristic peaks of arsenic, e.g., As 3d, As 3p, As 3 s and As LMM, can be detected in the As-loaded adsorbent, confirming the loading of As(V) on the material. The characteristic peaks for yttrium and iron such as Y 4p, Y 3d, Y 3p, Y 3 s and Fe 2p can be observed on the surface of virgin and As-loaded adsorbents. Furthermore, the high-resolution XPS spectrum of As 3d of the As-loaded adsorbent shown in Fig. 10 indicates that the main oxidation state of arsenic is + V and no reduction had occured [26].

The atomic ratios of virgin and As-loaded adsorbents are illustrated in Table 5 . After the adsorption, arsenic element is detected on the surface of the adsorbent with the atomic ratio of 3.71%. The atomic ratio of O decreases from 40.36 to 32.57% after the adsorption. This may be due to the replacement of functional groups on the adsorbent such as hydroxyl group and carbonate group by As(V).

The presence of carbonate group may cause additional removal of arsenic [6]. Though no carbonate was used during the adsorbent preparation, a certain amount of carbonate can be still introduced into the adsorbent form the atmosphere. Therefore, to further investigate the amount of carbonate group and its role in As(V) adsorption, the high-resolution C 1s spectra of virgin and As-loaded adsorbents were analyzed and the result is shown in Fig. 11.

The main absorption peak at 284.8 eV is assigned to the reference carbon that is from the atmosphere, while the peak at 290.31 eV corresponds to the carbonate group [27]. It is noted that the peak intensity of carbonate group significantly decreases from 10.28% to 5.46% after the adsorption. The exchange between the carbonate group and the As (V) is therefore deduced to occur during the adsorption.

As shown in Fig. 12, the O1s spectra before and after the As(V) adsorption are composed of three peaks respectively assigned to oxygen bonded to metal atom (M—O), hydroxyl group on metal atom (M—OH) and carbonate group ($-CO_3^{2-}$), and water molecular (H_2O). After the adsorption, the binding energies of the peaks are slightly altered due to the change of binding sites [28].

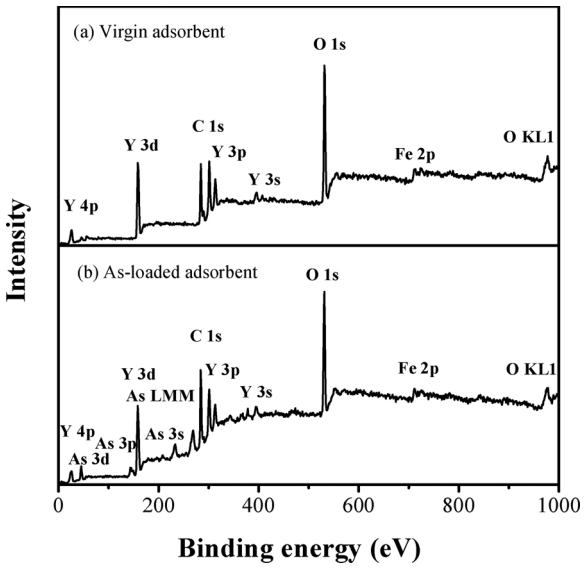

Fig. 9. XPS wide-scan spectra of adsorbents: (a) virgin adsorbent; (b) As-loaded adsorbent.

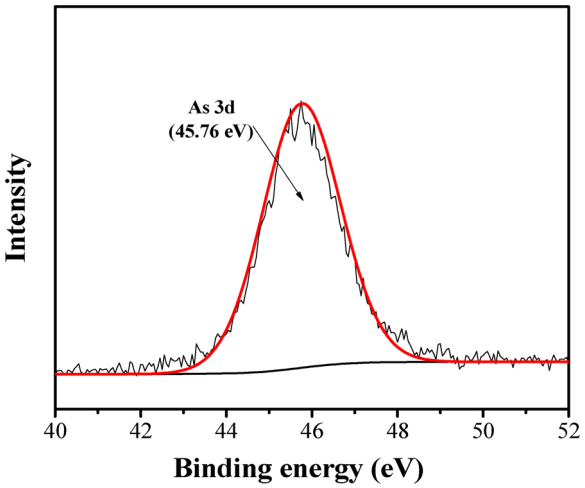

Fig. 10. XPS spectrum of As 3d of the As-loaded adsorbent.

Table 5
Atomic ratios of main elements in adsorbents from XPS study.

Atomic ratio (%)	Y	Fe	C	O	As
Virgin adsorbent	9.94	1.58	48.11	40.36	0
As-loaded adsorbent	9.04	1.63	52.98	32.57	3.71

Table 4
Adsorption capacities of the adsorbent towards As(V), phosphate and fluoride.

q (mg/g)	Initial conc. of phosphate (mM)				Initial conc. of fluoride (mM)			
	0	0.1	1.0	10	0	0.1	1.0	10
As	245.9	206.1	133.3	88.9	245.9	245.7	178.9	134.7
P	0	36.49	130.68	167.60	–	–	–	–
F	–	–	–	–	0	9.50	40.04	84.97

– refers to the absence of that anion in the solution.

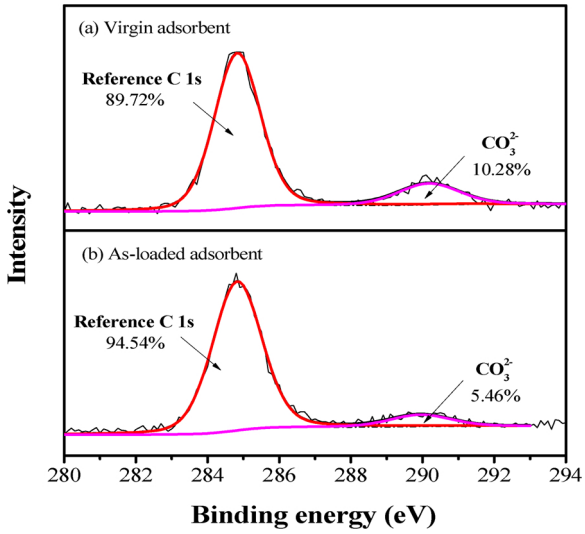

Fig. 11. XPS spectra of C 1s of adsorbents (a) before, and (b) after the As(V) adsorption.

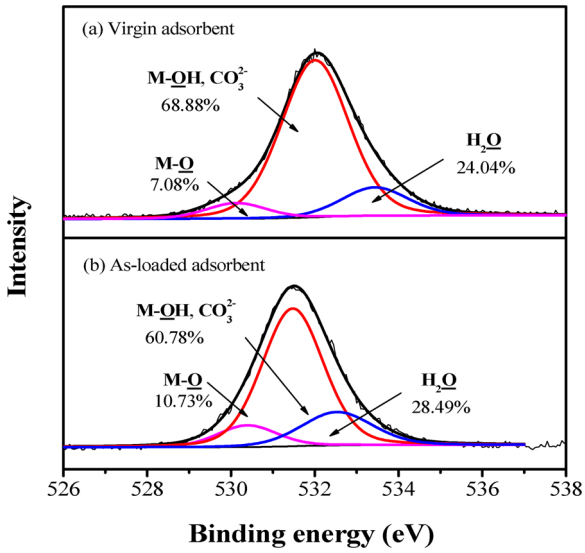

Fig. 12. XPS spectra of O 1s of adsorbents: (a) before, and (b) after the As(V) adsorption.

The relative contents of oxygen-containing groups are also shown in Fig. 12. The relative contents of M–O and H_2O respectively increase from 7.08% to 10.73% and 24.04% to 28.49% after the adsorption. Meanwhile, the amount of M−OH/$-CO_3^{2-}$ groups decreases from 68.88% to 60.78%. The change in the content of functional groups provides evidence for the involvement of hydroxyl group and carbonate group in the uptake of As(V) [5].

On the basis of atomic ratios shown in Table 5 and the percentages of functional groups, the chemical formula of the adsorbent is estimated as $Y_{13}Fe_2O_3(OH)_{27}(CO_3)_6{\cdot}12H_2O$.

3.6. Mechanism study

To further explore the mechanism of As(V) adsorption by the Y-Fe adsorbent, additional experiments were carried out. The Y-Fe adsorbent of different dosage was directly added into As(V) solution without the existence of other ions and one blank sample without As(V) was chosen as the reference. The solution pH, and the concentration changes in As (V), hydroxide and carbonate before and after the adsorption were measured.

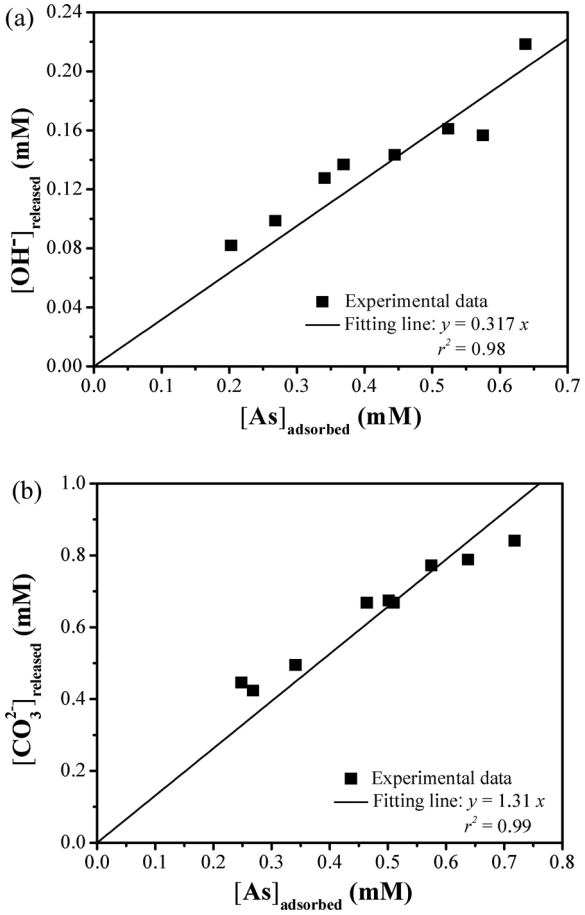

Fig. 13. The relationship between functional groups-released and As-adsorbed during adsorption process: (a) hydroxyl group, and (b) carbonate group.

There is a good linear relationship between hydroxide-released and As(V)-adsorbed (r^2 = 0.98) as shown in Fig. 13. The molar ratio of released hydroxide group ($[OH^-]_{released}$) and adsorbed As(V) ([As] adsorbed) in the adsorption process is about 0.317. Similarly, a good linear relationship is also observed between released carbonate and adsorbed As(V) with the correlation coefficient of 0.99; the molar ratio of $[CO_3^{2-}]$ released: [AS] adsorbed is about 1.31. This finding confirms that the functional groups on the adsorbent can be proportionally replaced by As(V) ions during the adsorption and the role of carbonate groups is of more importance for the As(V) adsorption than that of hydroxyl groups.

Furthermore, it explains the reasons why the uptake is very low at both pH 2 and 11. At pH 2, the carbonate species exist as carbonate acid and OH^- virtually does not exist. Hence, no uptake of arsenic can occur. At pH 11, the uptake is retarded due to the presence of too much OH^- in the solution.

4. Conclusions

The Y-Fe adsorbent was synthesized and applied to remove the highly concentrated As(V) form the simulated wastewater. The optimal adsorbent was obtained at the Y/Fe molar ratio of 8:1. The novel adsorbent was composed of aggregated nanoparticles and the pH_{PZC} of the adsorbent was around 7.0. A rapid uptake of As(V) can be achieved within the first 4 h and the adsorption equilibrium was obtained within 24 h. The optimal pH for As(V) adsorption was 4.0 and the maximum adsorption capacity at pH 4.0 and 7.0 could reach 401.8 and 288.7 mg-As/g, respectively. The results of ionic strength study indicated that the uptake of As(V) on the adsorbent was dominated by the inner-sphere

complex adsorption. The co-existing fluoride and phosphate ions showed significant interference on the adsorption of As(V). However, it exhibited potential for simultaneous removal of As(V), fluoride and phosphate. It was confirmed that the oxidation states of Y and Fe were mainly + III. Both hydroxyl and carbonate groups on the adsorbent surface played key roles in the uptake of arsenic through the ion exchange reactions.

Acknowledgments

The financial support from National Research Foundation Singapore (NRF2011NRF-POC001-028) is appreciated. Y.Y and L.Y. would like to thank the Singapore-Peking- Oxford Research Enterprise for providing the Ph.D scholarships under Grant COY-15-EWI-RCFSA/N197-1. Y.Y is grateful for the President's Graduate Fellowship provided by the National University of Singapore.

References

[1] B. Shi, J. Wang, H. Li, Y. Ma, L. Liang, L. Yang, C. Ma, X. Xu, Y. Xu, Y. Li, The survey of arsenic pollution in Yangzonghai Lake and its influence to the Yangzong River, the water source, the drinking water and local food in Yangzong Town of Yunnan Province, Chin. J. Endemiol. 33 (2014) 182–186.
[2] H. Cui, Q. Li, S. Gao, J.K. Shang, Strong adsorption of arsenic species by amorphous zirconium oxide nanoparticles, J. Ind. Eng. Chem. 18 (2012) 1418–1427.
[3] S. Tokunaga, S.A. Wasay, S.-W. Park, Removal of arsenic(V) ion from aqueous solutions by lanthanum compounds, Water Sci. Technol. 35 (1997) 71–78.
[4] Y. Zhang, M. Yang, X.-M. Dou, H. He, D.-S. Wang, Arsenate adsorption on an Fe – Ce bimetal oxide adsorbent: role of surface properties, Environ. Sci. Technol. 39 (2005) 7246–7253.
[5] D. Mohan, C.U. Pittman, Arsenic removal from water/wastewater using adsorbents—a critical review, J. Hazard. Mater. 142 (2007) 1–53.
[6] S.A. Wasay, M.J. Haron, A. Uchiumi, S. Tokunaga, Removal of arsenite and arsenate ions from aqueous solution by basic yttrium carbonate, Water Res. 30 (1996) 1143–1148.
[7] Z. Ren, G. Zhang, J. Paul Chen, Adsorptive removal of arsenic from water by an iron–zirconium binary oxide adsorbent, J. Colloid Interface Sci. 358 (2011) 230–237.
[8] C. Qin, L. Liu, Y. Han, C. Chen, Y. Lan, Mesoporous magnetic ferrum-yttrium binary oxide: a novel adsorbent for efficient arsenic removal from aqueous solution, Water Air Soil Pollut. 227 (2016) 337.
[9] G. Zhang, Z. Ren, X. Zhang, J. Chen, Nanostructured iron(III)-copper(II) binary oxide: a novel adsorbent for enhanced arsenic removal from aqueous solutions, Water Res. 47 (2013) 4022–4031.
[10] D. Kinniburgh, J. Syers, M. Jackson, Specific adsorption of trace amounts of calcium and strontium by hydrous oxides of iron and aluminum, Soil Sci. Soc. Am. J. 39 (1975) 464–470.
[11] J.F. Watts, J. Wolstenholme, An Introduction to Surface Analysis by XPS and AES, John Wiley & Sons, Ltd., 2005, pp. i–xi.
[12] S. Zhang, X.-Y. Li, J.P. Chen, Preparation and evaluation of a magnetite-doped activated carbon fiber for enhanced arsenic removal, Carbon 48 (2010) 60–67.
[13] G.M. Walker, L. Hansen, J.A. Hanna, S.J. Allen, Kinetics of a reactive dye adsorption onto dolomitic sorbents, Water Res. 37 (2003) 2081–2089.
[14] V. Vadivelan, K.V. Kumar, Equilibrium, kinetics, mechanism, and process design for the sorption of methylene blue onto rice husk, J. Colloid Interface Sci. 286 (2005) 90–100.
[15] M. Arami, N.Y. Limaee, N.M. Mahmoodi, Evaluation of the adsorption kinetics and equilibrium for the potential removal of acid dyes using a biosorbent, Chem. Eng. J. 139 (2008) 2–10.
[16] A.E. Ofomaja, Intraparticle diffusion process for lead(II) biosorption onto mansonia wood sawdust, Bioresour. Technol. 101 (2010) 5868–5876.
[17] Y. Yu, L. Yu, M. Sun, J.P. Chen, Facile synthesis of highly active hydrated yttrium oxide towards arsenate adsorption, J. Colloid Interface Sci. 474 (2016) 216–222.
[18] Y.-M. Zheng, S.-F. Lim, J.P. Chen, Preparation and characterization of zirconium-based magnetic sorbent for arsenate removal, J. Colloid Interface Sci. 338 (2009) 22–29.
[19] K.F. Hayes, C. Papelis, J.O. Leckie, Modeling ionic strength effects on anion adsorption at hydrous oxide/solution interfaces, J. Colloid Interface Sci. 125 (1988) 717–726.
[20] Y.-T. Wei, Y.-M. Zheng, J. Paul Chen, Enhanced adsorption of arsenate onto a natural polymer-based sorbent by surface atom transfer radical polymerization, J. Colloid Interface Sci. 356 (2011) 234–239.
[21] G.-S. Zhang, J.-H. Qu, H.-J. Liu, R.-P. Liu, G.-T. Li, Removal mechanism of As(III) by a novel Fe – Mn binary oxide adsorbent: oxidation and sorption, Environ. Sci. Technol. 41 (2007) 4613–4619.
[22] Y. Ma, Y.-M. Zheng, J.P. Chen, A zirconium based nanoparticle for significantly enhanced adsorption of arsenate: synthesis, characterization and performance, J. Colloid Interface Sci. 354 (2011) 785–792.
[23] T. Wen, X. Wu, X. Tan, X. Wang, A. Xu, One-pot synthesis of water-swellable Mg–Al layered double hydroxides and graphene oxide nanocomposites for efficient removal of As(V) from aqueous solutions, ACS Appl. Mater. Interfaces 5 (2013) 3304–3311.
[24] K. Gupta, U.C. Ghosh, Arsenic removal using hydrous nanostructure iron (III)–titanium(IV) binary mixed oxide from aqueous solution, J. Hazard. Mater. 161 (2009) 884–892.
[25] R. Chen, C. Zhi, H. Yang, Y. Bando, Z. Zhang, N. Sugiur, D. Golberg, Arsenic (V) adsorption on Fe_3O_4 nanoparticle-coated boron nitride nanotubes, J. Colloid Interface Sci. 359 (2011) 261–268.
[26] W.J. Stec, W.E. Morgan, R.G. Albridge, J.R. Van Wazer, Measured binding energy shifts of "3p" and "3d" electrons in arsenic compounds, Inorg. Chem. 11 (1972) 219–225.
[27] J.K. Heuer, J.F. Stubbins, An XPS characterization of $FeCO_3$ films from CO_2 corrosion, Corros. Sci. 41 (1999) 1231–1243.
[28] S. Gudmundsdottir, E. Skulason, K.-J. Weststrate, L. Juurlink, H. Jonsson, Hydrogen adsorption and desorption at the Pt(110)-(1[times]2) surface: experimental and theoretical study, J. Chem. Soc. Faraday Trans. 15 (2013) 6323–6332.